The transition between Makran subduction and the Zagros collision: recent advances in its structure and active deformation

V. REGARD[1]*, D. HATZFELD[2], M. MOLINARO[3,4], C. AUBOURG[3], R. BAYER[5], O. BELLIER[6], F. YAMINI-FARD[7], M. PEYRET[5] & M. ABBASSI[7]

[1]*LMTG, Université de Toulouse–CNRS–IRD–OMP, 14 av. E. Belin, 31400 Toulouse, France*

[2]*LGIT, Maison des Géosciences, BP 53, 38400 Grenoble Cedex 9, France*

[3]*Laboratoire de Tectonique, CNRS, Université de Cergy-Pontoise, Cergy, France*

[4]*Present address: Shell International Exploration and Production B.V., Rijswijk, Netherlands*

[5]*Géosciences Montpellier, UMR 5243–CC 60, Université Montpellier 2, Place E. Bataillon, 34095 Montpellier cedex 5, France*

[6]*CEREGE, Aix–Marseille Université–CNRS & IRD, Europôle Méditerranéen Arbois, F-13545 Aix-en-Provence, France*

[7]*International Institute of Earthquake Engineering and Seismology, Tehran, Iran*

**Corresponding author (e-mail: regard@lmtg.obs-mip.fr)*

Abstract: SE Iran is the site of a rare case of young transition between subduction and collision. We have synthesized recent results in geodesy, tectonics, seismology and magnetism to help understand the structure and kinematics of the Zagros–Makran transition. Surface observations (tectonics, magnetism and geodesy) indicate a transpressive discontinuity consisting of several faults striking obliquely to the convergent plate motion, whereas deeper observations (seismology) support a smooth transition across the fault system. No lithospheric transform fault has been created, although the transition already behaves like a major boundary in terms of tectonic style, seismic structure, lithology and magnetism. The Zendan–Minab–Palami fault system consists of several faults that accommodate a transpressive tectonic regime. It is the surface expression of a southward propagation of the north–south-trending right-lateral strike-slip fault system of Jiroft–Sabzevaran. Within each system the numerous faults will coalesce into a single, lithospheric, wrench fault.

The spatial transition between subduction and continental collision is by itself unstable and often a transform fault will develop to accommodate the differences in tectonic setting, as the Chaman Fault in central Asia does (Lawrence *et al.* 1992). Interestingly, the Hormuz Strait area in Iran (26.58N, 56.58E, Fig. 1) displays such a setting, but in a juvenile stage. At this point Arabia converges northward with Eurasia at a velocity of 23–25 mm a^{21} according to global positioning system (GPS) measurements (Bayer *et al.* 2003, 2006; McClusky *et al.* 2003; Vernant *et al.* 2004; Masson *et al.* 2007). The Arabian plate is oceanic to the east in the Oman Gulf whereas it is continental to the west in the Arabian platform (Fig. 1). As expected, the Arabian and Eurasian continental plates collide to the west, forming the NW–SE-striking Zagros fold-and-thrust belt (ZFTB), which is a continental accretionary prism within the Arabian plate and accommodates about 10 mm a^{21} of NNE–SSW-trending shortening (Alavi 1994; Talebian & Jackson 2002; Tatar *et al.* 2002; Blanc *et al.* 2003). To the east, Arabia subducts under Iran, resulting in an extensive accretionary prism, of which the east–west-striking Makran belt is the emerged portion (Byrne *et al.* 1992; McCall 1997; Kopp *et al.* 2000). Between these regions, the structures in the Hormuz area define a curved structure connecting the Main Zagros Thrust (MZT) suture to the Makran frontal thrust (Fig. 1); this curved structure probably represents the newly formed transform fault. These structures connecting the Zagros and Makran mountain belts trend north–south to NNW–SSE, and are therefore highly oblique to the north–south convergence velocity, with an expected transpressive character.

This area has been studied for some time by geologists and geophysicists. The latter have described a sharp boundary between the eastern and western domains called the 'Oman Line'. Despite

From: Leturmy, P. & Robin, C. (eds) *Tectonic and Stratigraphic Evolution of Zagros and Makran during the Mesozoic–Cenozoic*. Geological Society, London, Special Publications, 330, 43–64.
DOI: 10.1144/SP330.4 0305-8719/10/$15.00

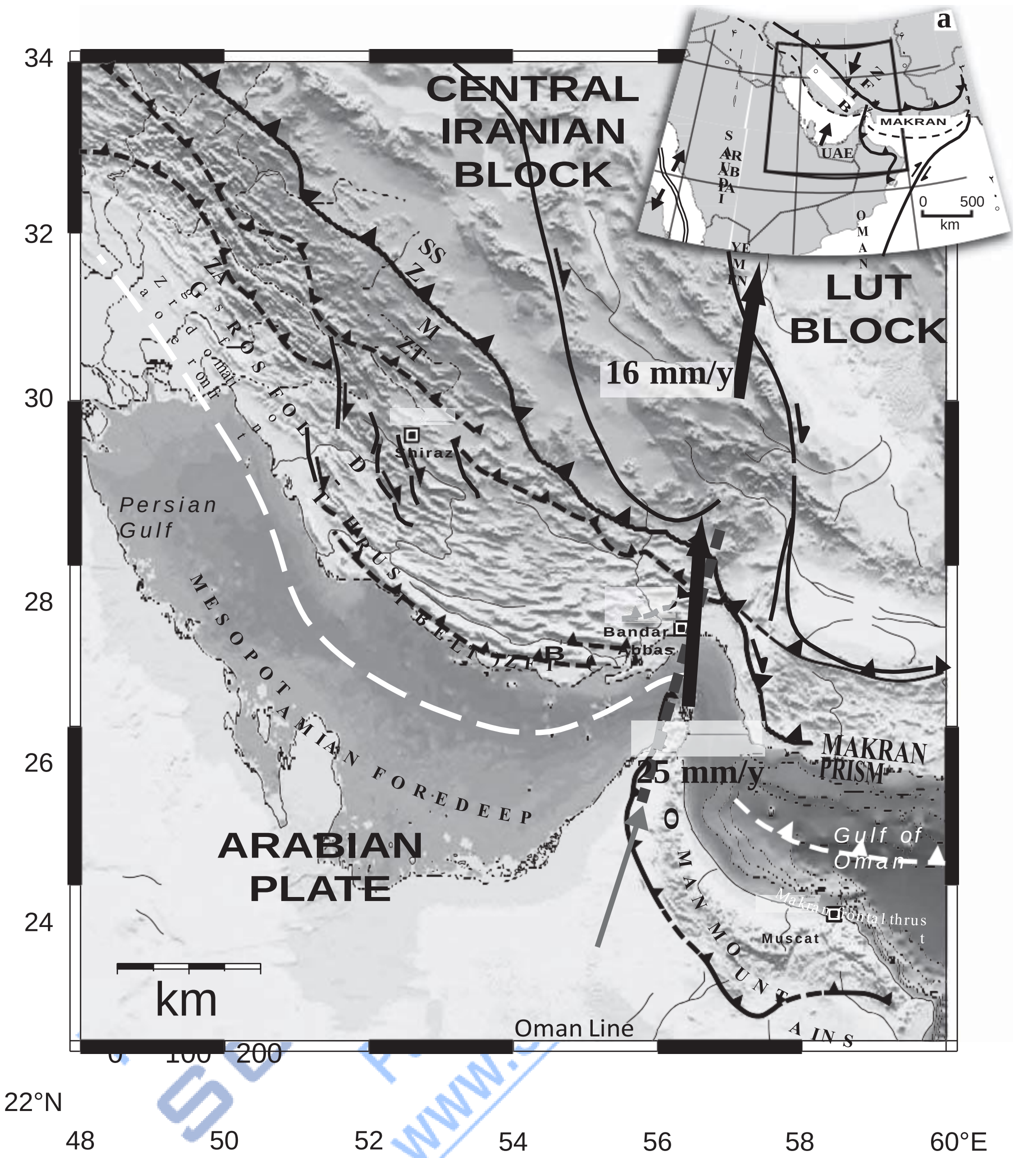

Fig. 1. Map of South Iran–North Arabia (modified after Molinaro *et al.* 2005*a*). The arrows represent the velocity relative to Eurasia (Vernant *et al.* 2004). It should be noted that the convergence accommodated through the Zagros Fold-and-Thrust Belt (ZFTB) is only *c.* 9 mm a^{21}, and there is no value currently available for the part of the Arabia–Eurasia convergence accommodated through the Makran between Arabia and Lut [except using the Vernant *et al.* (2004) results with some assumptions]. MZT, Main Zagros Thrust; SSZ, Sanandaj–Sirjan Zone.

the associated low seismicity its sharpness was interpreted as evidence of a transform fault (Kadinsky-Cade & Barazangi 1982).

To provide a better understanding of this newly evolving transform fault system, the area has been recently studied using various geological and geophysical techniques, in the framework of an Iranian–French collaboration, including palaeomagnetism (Aubourg *et al.* 2004, 2008; Smith *et al.* 2005), Tertiary and active tectonics (Molinaro *et al.* 2004, 2005*a*; Regard *et al.* 2004, 2005*a*), seismology (Yamini-Fard 2003; Yamini-Fard & Hatzfeld 2008), and geodesy (Vernant *et al.* 2004; Bayer *et al.* 2006; Masson *et al.* 2007). The purpose of this paper is to provide a synthesis of these acquired data and to discuss this subduction–collision transition. Thus, after introducing the general setting of the area, the present-day and recent deformation, and the upper crustal structure from balanced cross-sections, we discuss the deep crustal structure revealed by seismological studies and finally present the actual deformation rates from GPS and geodesy.

Geological setting

Zagros

The Zagros mountain belt is a NW–SE-trending fold-and-thrust belt, consisting of a 6–15 km thick sedimentary pile that overlies Precambrian metamorphic basement (McCall *et al.* 1985; McCall 1997). The sedimentary cover can be divided into three successive sequences. At its base, it is composed of thick late Precambrian evaporitic deposits (the so-called 'Hormuz Salt'), which constitute the main regional décollement for most of the larger folds within the Zagros fold-and-thrust belt (ZFTB). This layer is the origin of numerous salt diapirs that have pierced the overlying sedimentary cover and risen to the surface. A *c.* 4000 m thick Cambrian to Eocene sequence forms the so-called Competent Group. Apart from the initial Cambrian–Carboniferous clastic formations, the majority of this group until the Upper Cretaceous units consists of massive platform carbonate rocks (James & Wynd 1965; Faure-Muret & Choubert 1971; Szabo & Kheradpir 1978; Sharland *et al.* 2001). The remainder of the stratigraphic sequence is represented by the Miocene to Recent clastic sediments of the Incompetent Group. These molasse-type sediments, derived from the uplift and erosion of the Zagros Mountains, show a typical coarsening-up evolution from marine-to-continental clastic deposits to coarse proximal conglomerates at the top (James & Wynd 1965; Edgell 1996; Hessami *et al.* 2001).

Makran

The Makran accretionary wedge stretches from Iran to central Pakistan and extends off the south coast of this region (Schluter *et al.* 2002). It has been formed by the subduction of the oceanic portion of the Arabian plate beneath Eurasia and is built up by sediments scraped off the Arabian plate since the early Tertiary (Berberian & King 1981; Harms *et al.* 1984; Kopp *et al.* 2000). Subduction was probably initiated during Palaeocene time (Platt *et al.* 1988) and accretion started during Eocene time (Byrne *et al.* 1992). The modern Makran accretionary prism has developed since the Late Miocene (Platt *et al.* 1985, 1988), and is still propagating seaward at a rate of *c.* 10 mm a^{21} (White 1982). Two features make this accretionary wedge unusual: (1) the sediment thickness on top of the oceanic crust is extremely high (at least 6 km); (2) the dip angle of subduction is extremely low (*c.* 58, Jacob & Quittmeyer 1979; Byrne *et al.* 1992; Carbon 1996).

Zagros–Makran transition

The Zagros and Makran domains are both bounded to the north by a continuous ophiolitic belt along the Main Zagros reverse fault and its eastern continuation along the Makran Thrust (Fig. 1) (McCall 1997). South of this suture, the Zagros and Makran regions behave differently, highlighting how the subduction and collision settings differ. Whereas the convergence velocity accommodated by the Zagros collision increases progressively from NW to SE, the transition from the collision to the Makran subduction is marked by a jump from 9 + 2 to *c.* 19 + 2 mm a^{21} (Vernant *et al.* 2004; Masson *et al.* 2007). The Zagros–Makran transition is thus expected to have a wrench motion of at least some 10 mm a^{21}. During the late Cenozoic, Arabia and Eurasia continuously converged (Fig. 2; McQuarrie *et al.* 2003). Palinspastic reconstructions show how this continuous convergence was accommodated in the Zagros and Makran during the last 30 Ma (Fig. 2), suggesting that the Zagros–Makran transition zone must have been formed during the last *c.* 15 Ma.

The transition takes place at the front of the mountainous Musandam peninsula (Hormuz Strait, Fig. 1). Formed during the Late Cretaceous, this mountain range not only magnifies the differences between the continent and the ocean, but also acts as a heterogeneity within the colliding Arabia plate. It can be traced up to the Hormuz Strait, in a seismic profile running from Qeshm to Minab (Ross *et al.* 1986). Such a set-up suggests that the Oman peninsula may have interfered with the Zagros collision and be partly responsible for the curved shape of the Zagros–Makran transition (Ricou *et al.* 1977; Kadinsky-Cade & Barazangi 1982; Aubourg *et al.* 2008). Several other mechanisms have been proposed to explain this curved shape of the Fars Arc: (1) rotation of basement faults (Hessami *et al.* 2001); (2) a change in the style of accommodation of shortening from head-on shortening in the SE to oblique shortening to the NW of the ZFTB, observed by Talebian & Jackson (2004); (3) a Jura style of deformation in which the arcuate shape is controlled by the pro- gressive lateral pinch-out of the basal Hormuz evap- orates upon which the Zagros folds detach (Molinaro *et al.* 2005*a*).

The transition between the Zagros and Makran is also often described in the literature as the 'Oman Line' trending N208E and running northward from the Musandam peninsula (Kadinsky-Cade &

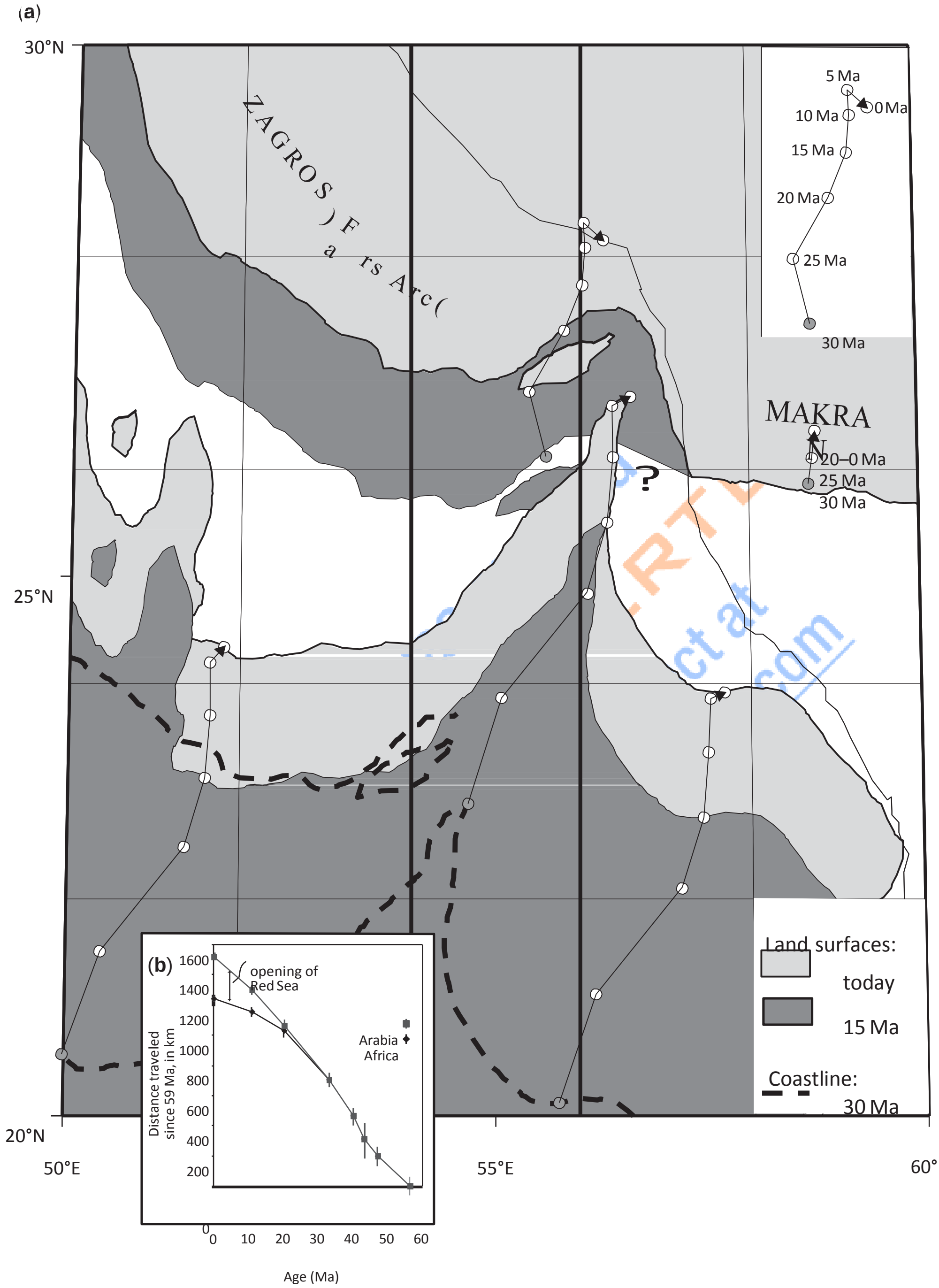

Fig. 2. (a) Palinspastic reconstructions around the study area for the last 30 Ma, with plates moving relative to Eurasia. The segmented lines with circles represent the displacement trajectories (see inset for stages). The reconstruction is according to the ODSN Plate Tectonic Reconstruction Service (http://www.odsn.de/odsn/services/paleomap/paleomap.html). Reconstructions are based on block rotations calculated from magnetic anomalies (Hay *et al.* 1999; Soeding 1999). The ancient Makran shoreline cannot be estimated as it is formed by an accretionary prism under construction; the motion-segmented arrow is estimated by the Lut block reconstructed position. (b) Graph showing the position of a reference point (388N, 488E) representing Arabia with respect to Eurasia v. time, both including (grey boxes) and excluding (black diamonds) rotation describing the opening of the Red Sea, modified after McQuarrie *et al.* (2003).

Barazangi 1982). It separates the continent to the east from the Oman Gulf oceanic crust to the west; it represents an inactive transform zone inher- ited from the Neotethys ocean opening (White & Ross 1979). This transition marks the boundary between a region of high seismicity located in the NW (the Zagros domain) and a region of low seismi- city to the east, and is highlighted by the Musandam peninsula trend. Formerly the Oman Line was suggested to represent the transition between the Zagros and Makran (Kadinsky-Cade & Barazangi 1982), but it is now thought that this role is played by the Minab – Zendan Fault system, whose southern prolongation has been seen on seismic pro- files from the Oman Gulf (Ravaut *et al.* 1998).

The multidisciplinary study presented here aims at better determining the structure and kinematics of this key area. In particular, the Zendan–Minab Fault system (Fig. 3) is studied to help us understand why, as it seems to play a major role in the accom- modation of the deformation, the associated seis- micity is low. We also discuss the deformation related to this zone and see if it could be the result of the indentation by the Musandam peninsula.

Results

Deformation pattern

Tectonics. Using satellite images, and structural and geomorphological field observations, Regard *et al.* (2004) illustrated the study area's present-day deformation pattern accommodated by faulting. The study area shows a distributed deformation

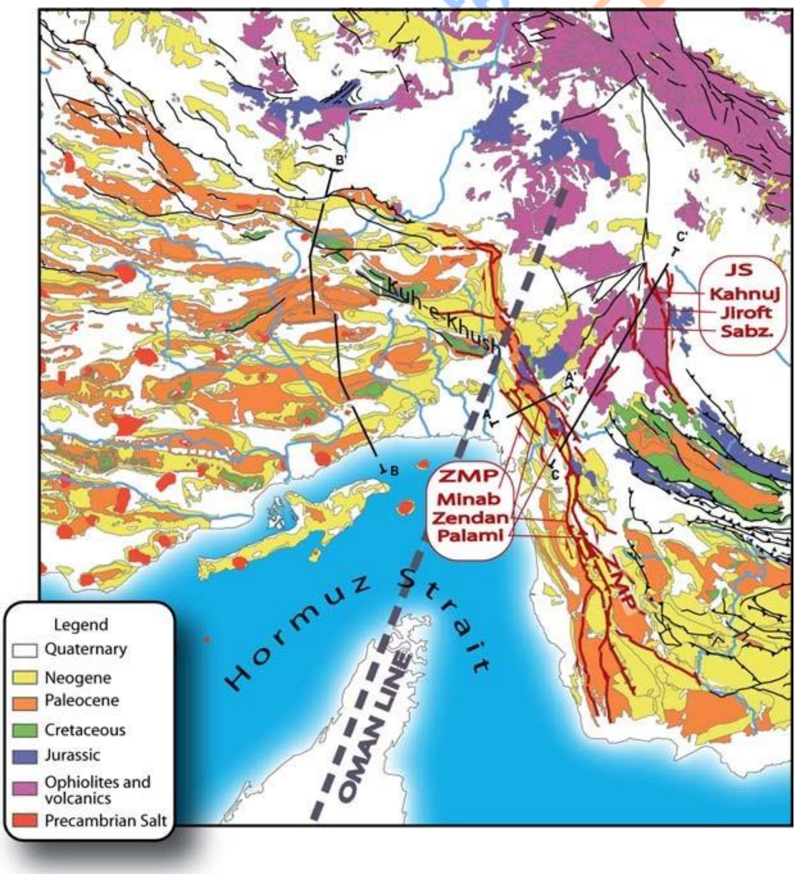

Fig. 3. Geological map of the study area, modified from the 1:1 000 000 geological map of Iran. Faults in black are those from the original drawing; faults in red are the active faults mapped by Regard *et al.* (2004), which are distributed in two fault systems: (1) the Jiroft, Sabzevaran (abbreviated as Sabz.) and Kahnuj faults in the Jiroft–Sabzevaran fault system (JS); (2) the Minab, Zendan and Palami faults in the Zendan–Minab–Palami fault system (ZMP). A–A′ and B–B′ are the cross-sections (Fig. 5) from Molinaro *et al.* (2004). C–C′ is the local tomography cross-section (Fig. 8), from Yamini-Fard *et al.* (2007).

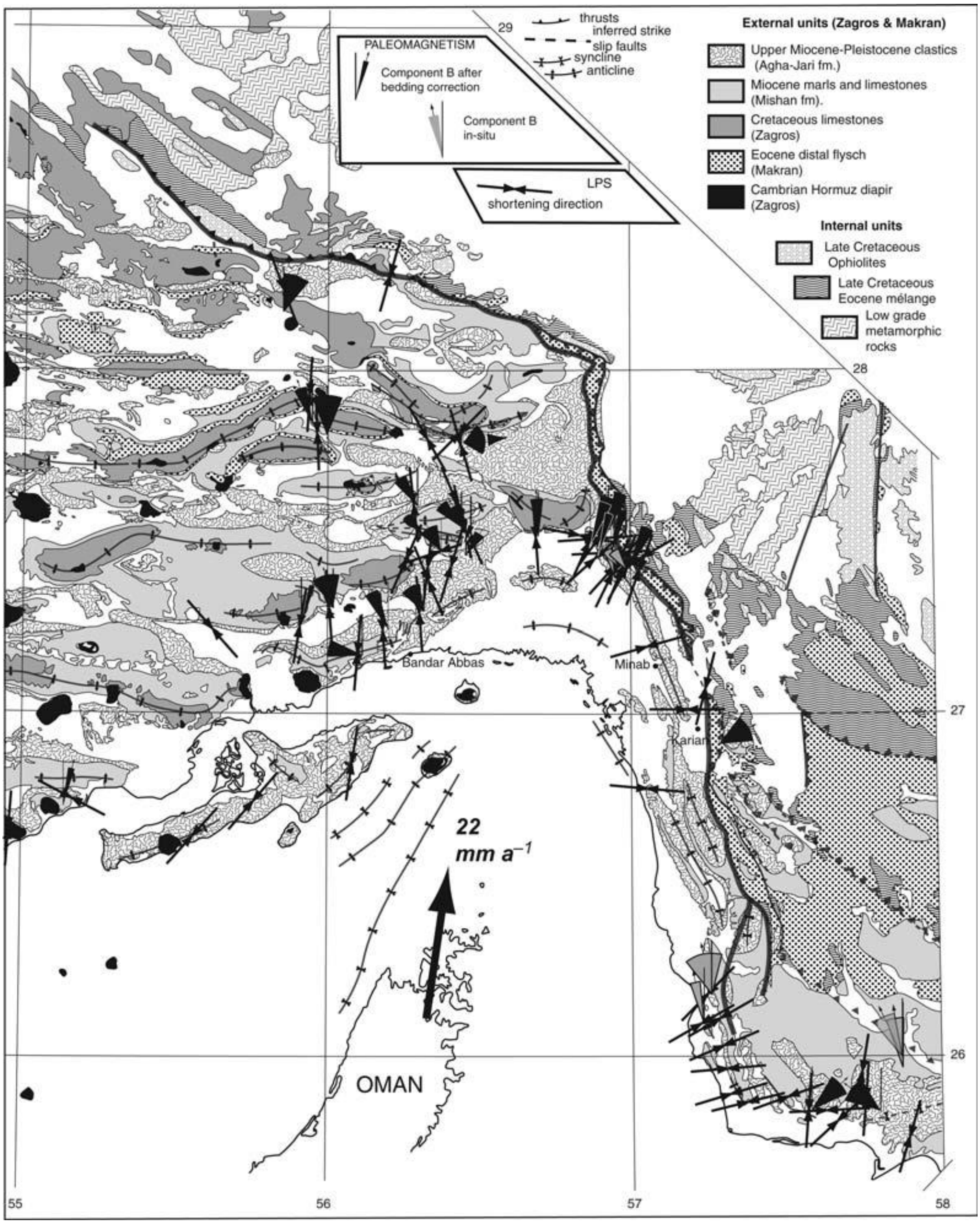

Fig. 4. Summary of magnetic studies on the Fars Arc and western Makran (Bakhtari *et al.* 1998; Aubourg *et al.* 2004; Smith *et al.* 2005).

pattern covering a wide domain (Fig. 3). Six north–south- to NW–SE-trending major faults were identified, each displaying clear evidence of late Quaternary reverse right-lateral slip. They constitute two fault systems. The first one encompasses, from west to east, the Minab, Zendan and Palami faults (the ZMP fault system; Fig. 3). The Zendan Fault corresponds to the lithological boundary between the Zagros and Makran. The second one, the Jiroft–Sabzevaran (JS) fault system, comprises the Jiroft, Kahnuj and Sabzevaran north–south-trending faults (Fig. 3). The ZMP fault system transfers the Zagros (continental prism) deformation to the Makran accretionary prism, whereas the JS fault system transfers some motion northward to the Alborz–Kopet Dagh convergence zone in northern Iran (Figs 1 & 3). Tectonic study and fault slip vector analyses indicate that two distinct tectonic regimes have occurred successively since the Miocene within a consistent regional NE–SW-trending compression: (1) a late Miocene to Pliocene tectonic regime characterized by partitioning between reverse faulting and en echelon folding; (2) a NE–SW-trending σ_1 axis transpressional regime homogeneously affecting the region since the late Pliocene (Regard *et al.* 2004). The change is contemporaneous with a major regional tectonic reorganization (Allen *et al.* 2004). This study provides evidence of active deformation that is not localized, but is distributed across a wide zone. It accommodates the convergence and transfers it from collision to subduction by transpressional tectonics without any partitioning process in the present-day period.

Magnetism. Several studies using magnetic fabric data were conducted in the Fars Arc and in the eastern Makran (Bakhtari *et al.* 1998; Aubourg & Robion 2002; Aubourg *et al.* 2004; Smith *et al.* 2005). In the Agha-Jari formation (Upper Miocene–Pleistocene silicoclastic rocks), the magnetic foliation is parallel to the bedding, whereas the magnetic lineation strikes perpendicular to the horizontal shortening or layer-parallel shortening (LPS). Several studies from other thrust belts (e.g. in the Pyrenees, Averbuch *et al.* 1992; Pares *et al.* 1999) suggest that the magnetic lineation records LPS that occurs before any detectable folding.

Near our study area, Aubourg *et al.* (2004) compared the magnetic fabric data with P-axis earthquake focal mechanisms and found a good agreement west of the Zagros–Makran transition, contrasting with significant differences in the east. Data collected during the last 10 years are summarized in Figure 4. To the west, in the Fars Arc, the general trend is a shortening direction (LPS) close to the GPS convergence direction (north–south), with slight anticlockwise rotations. Just west of and within the Minab–Zendan fault system, the shortening direction is roughly normal to the structures whereas clockwise rotations are recorded. To the east (within the Makran), data are sparse and do not show a clear signal, despite much LPS directed parallel to the north–south convergence direction.

Smith *et al.* (2005) and Aubourg *et al.* (2008) measured palaeomagnetic data in the Agha-Jari formation (Mio-Pliocene) to document vertical-axis block rotations. The pre-tilting palaeomagnetic component B documents the rotation that occurred between the age of Agha-Jari Fm. and recent time (Fig. 4). At first glance, it is apparent that clockwise and counterclockwise rotations of small magnitude (typically less than 208) occurred respectively in the eastern and western Zagros–Makran transition zone. If the block rotation is removed, the LPS directions are in good agreement with the overall convergence direction. This suggests that the present shape of the Zagros–Makran transition zone, oblique to the convergence direction, has been acquired only recently (since Mio-Pliocene time).

Together, the palaeomagnetic and magnetic fabric data (LPS) document the roughly north–south convergence, except near the Zagros–Makran transition zone, where the structures have experienced recent clockwise rotations that may continue at present (Fig. 4). These rotations agree with a wrench zone that is not localized on a single structure but extends over an area that is some tens of kilometres wide. The Fars Arc exhibits slight anticlockwise rotations, suggesting it has experienced some indentation since Middle Miocene time (Fig. 4).

Balanced cross-sections

Molinaro *et al.* constructed two cross-sections on each side of the Zagros–Makran transition (Molinaro *et al.* 2004, 2005*a*). The contribution of that work is not only to provide quantitative shortening values but also to reveal how the deformation is accommodated. The section on the eastern side of the transition indicates some 6 km of shortening in front of the Zendan Fault, affecting only the Tertiary cover, over a décollement *c.* 6 km deep (Fig. 5; section AA′ in Fig. 3). The shortening is measured perpendicular to the Zendan Fault (i.e. along a N1508E trend). In the SE Zagros, the Bandar Abbas–Hadjiabad section (BB′ in Fig. 3) displays two different north–south shortening values of 10 and 45 km, respectively, for the basement and the cover (Fig. 5). In particular, with this section Molinaro *et al.* documented two main steps in the evolution of the Zagros fold–thrust belt. In the first (Mio-Pliocene) stage the deformation was thin-skinned in style, with a décollement at *c.* 8–9 km depth. In the second (Pliocene to Recent) shortening stage, the basement must be involved through major thrust faults, inferred from focal mechanisms and observation of steps in the general topography and structural elevation of the Zagros mountains. These faults ramp up through the cover and cut the former folds obliquely; the best example is the Kuh-e-Khush (Fig. 2). This obli- quity could be due to rotation of folds, reactivation of old basement structures or stress rotation. Geographically, to the west, in the Zagros, deformation involves the entire crust, with folding in the cover controlled by the basal Hormuz Salt layer and

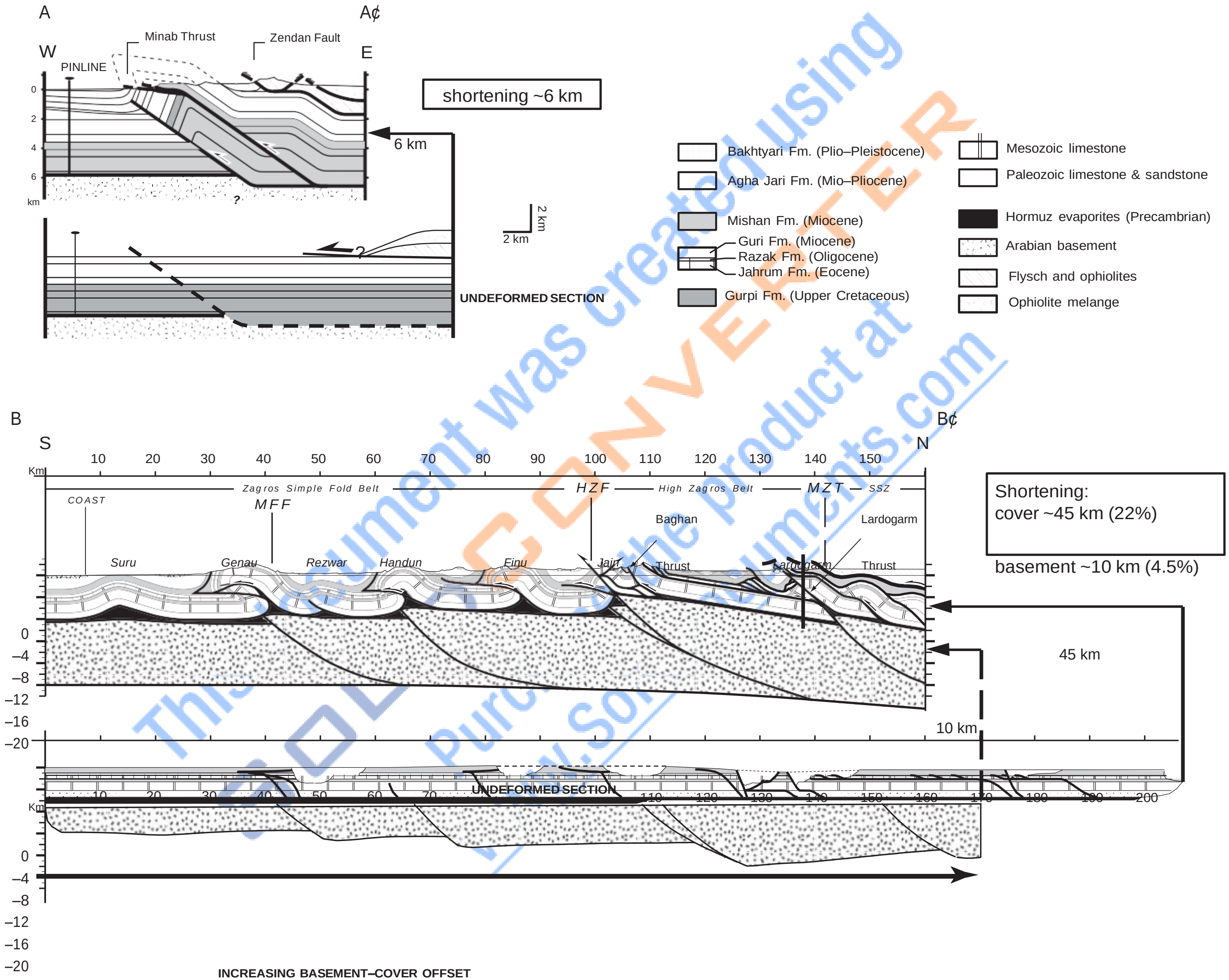
A
A¢
W
E
Minab Thrust
Zendan Fault
PINLINE
0
2
4
6
km
?
shortening ~6 km
6 km
2 km
2 km
UNDEFORMED SECTION
Bakhtyari Fm. (Plio–Pleistocene)
Agha Jari Fm. (Mio–Pliocene)
Mishan Fm. (Miocene)
Guri Fm. (Miocene)
Razak Fm. (Oligocene)
Jahrum Fm. (Eocene)
Gurpi Fm. (Upper Cretaceous)
Mesozoic limestone
Paleozoic limestone & sandstone
Hormuz evaporites (Precambrian)
Arabian basement
Flysch and ophiolites
Ophiolite melange
B
B¢
S
N
Km
10 20 30 40 50 60 70 80 90 100 110 120 130 140 150
Zagros Simple Fold Belt
HZF
High Zagros Belt
MZT
SSZ
COAST
MFF
Baghan
Lardogarm
Suru
Genau
Rezwar
Handun
Finu
Jain
Thrust
Lardogarm
Thrust
Shortening:
cover ~45 km (22%)
basement ~10 km (4.5%)
45 km
10 km
0
–4
–8
–12
–16
–20
UNDEFORMED SECTION
10 20 30 40 50 60 70 80 90 100 110 120 130 140 150 160 170 180 190 200
INCREASING BASEMENT–COVER OFFSET

Fig. 5. Balanced cross-sections, from Molinaro *et al*. (2004, 2005*a*). (See Fig. 3 for profile location.) A–A′, cross-section through the Minab–Zendan fault system; B–B′, cross-section from Bandar Abbas to Hajiabad, southeastern Zagros. MFF, Main Front Fault; HZF, High Zagros Fault; MZT, Main Zagros Thrust; SSZ, Sanandaj–Sirjan Zone.

major thrusting in the basement. To the east, on the other hand, folding is controlled by a décollement located at 6 km depth and the basement does not appear to be involved in the deformation.

Seismotectonics and deep structure

Seismotectonics. Yamini-Fard *et al*. (2007) installed a dense seismological mobile network of 24 stations for 8 weeks in 1999, in the area of Bandar Abbas, to locate precisely the microseismicity of the area and calculate focal mechanisms (Fig. 6). In addition, they carried out a tomographic traverse, with 25 stations from Hadjiabad to Minab and the Makran ranges (Fig. 7).

The microearthquake distribution around the transition between the Zagros continental collision and the Makran subduction is restricted to the west

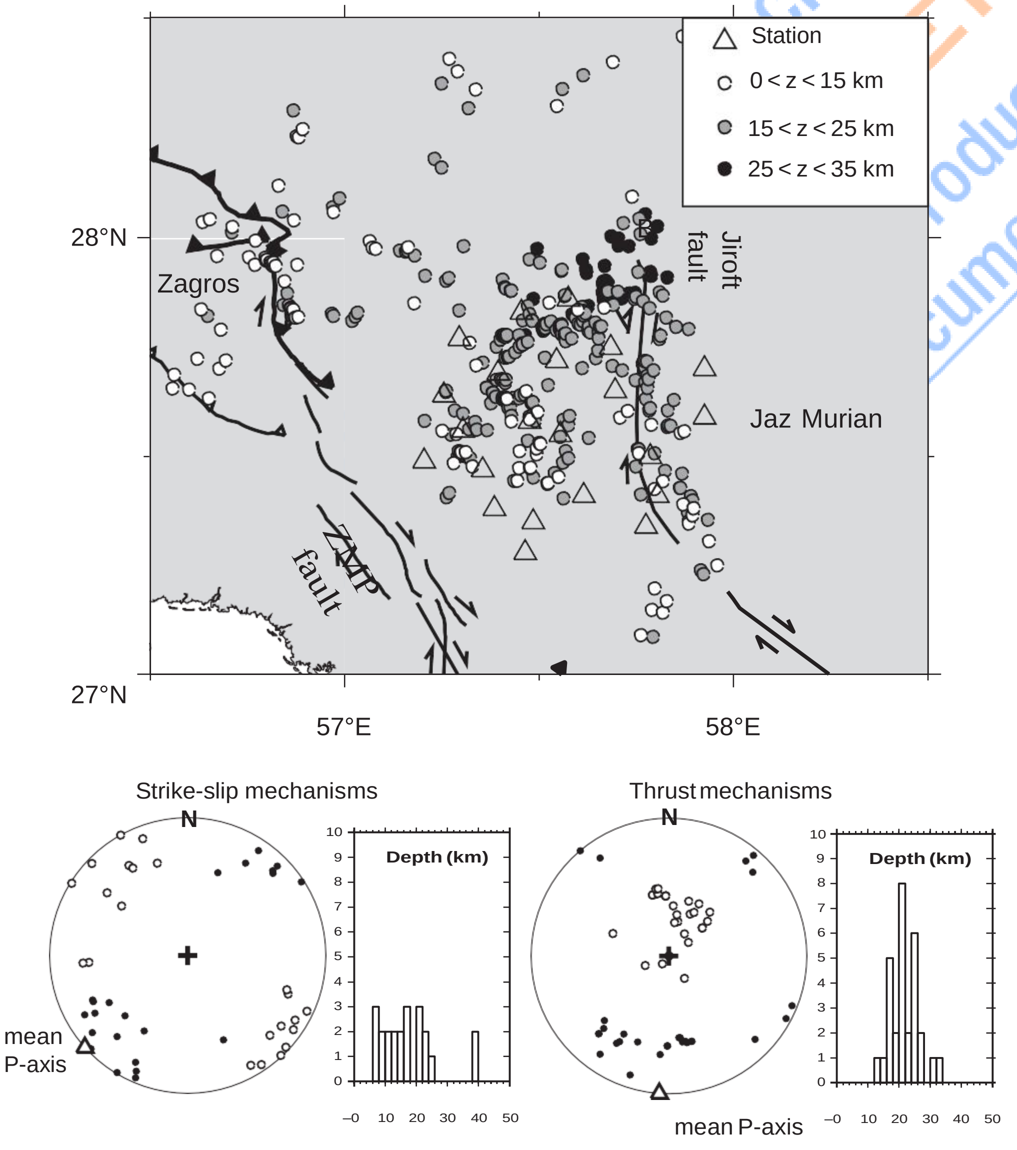

Fig. 6. Map of the microseismicity recorded for the period 17 November 1999 to 6 January 2000 by Yamini-Fard (2003) and Yamini-Fard *et al*. (2007). They computed 59 focal mechanisms that can be divided into two groups in terms of their mechanism: strike-slip (horizontal T-axis) or thrusting (vertical T-axis). These lead, respectively, to a *c*. N458E-trending and roughly north-trending mean P-axis. Interestingly, thrust mechanisms occur at depths (15–35 km) greater than strike-slip mechanisms (5–25 km); filled and open circles are P- and T-axes, respectively (redrawn after Yamini-Fard *et al*. 2007).

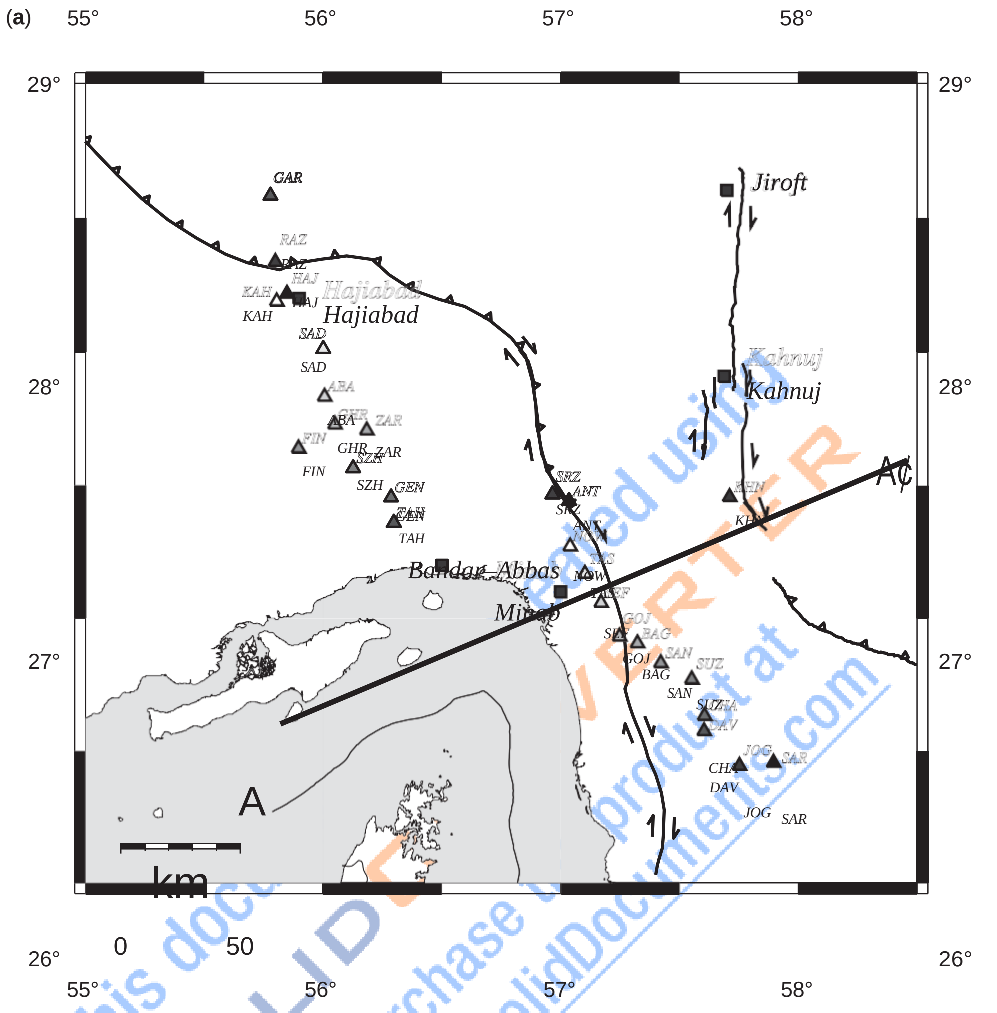

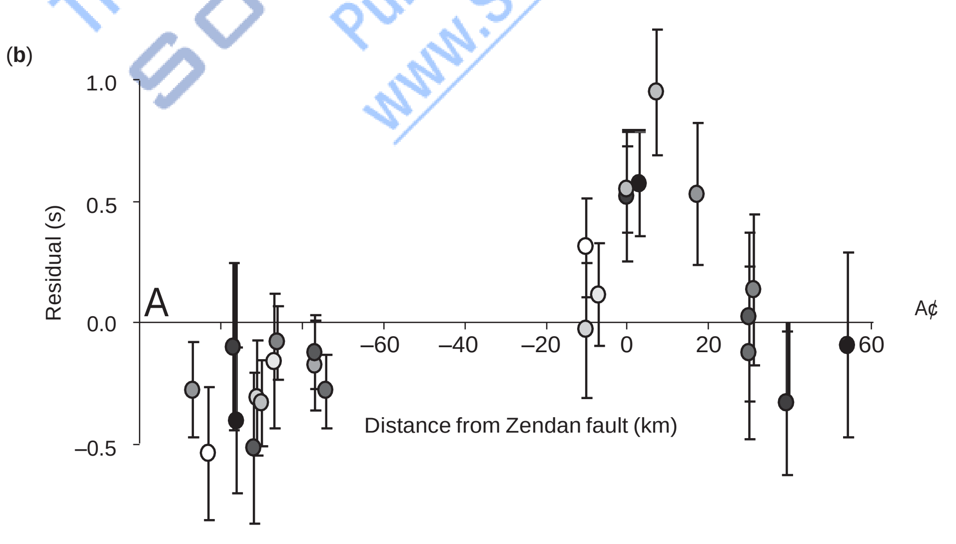

Fig. 7. Teleseismic travel-times residuals at stations along the Minab profile. (a) Location of seismological stations. (b) Residual values, given by reference to the average residual (in s) v. eastward distance to the Zendan Fault. Redrawn

from Yamini-Fard (2003) and Yamini-Fard & Hatzfeld (2008). Corresponding symbol shades are used in the map and the residual graph.

of the Jaz Murian depression and the Jiroft Fault (Fig. 6). No earthquakes seem to be related to the Zendan–Minab–Palami fault system. Most of the shallow seismicity is related either to the Zagros mountain belt, located to the west, or to the Sabzevaran–Jiroft fault system, located to the north. The depth distribution of the microearthquakes increases northeastward to an unusual value for the Zagros of 40 km. Two dominant types of focal mechanisms are observed in this region: low-angle thrust mostly restricted to the lower crust (at depths between 15 and 30 km) and strike-slip at shallow depth (10–20 km, Fig. 6). Both are consistent with north–south to NE–SW shortening.

Crustal seismic structure. Teleseismic P-wave travel times, from *c*. 50 earthquakes, were calculated along a profile that crosses the Minab–Zendan fault system at three locations. The orientation of the profile was governed by accessibility and safety of the road. We observe a large delay in the travel time residual every time the profile crosses the ZMP fault system (Fig. 7). The inversion of the travel time residuals performed by Yamini-Fard (2003) highlights perturbations relative to a homogeneously layered velocity structure. In the first layer (associated with the crust), two low-velocity anomalies are related to the ZMP fault zone. The deeper layers related to the upper mantle show a slow velocity in the west relative to a fast velocity in the east of the ZMP fault system. If we project the residual on a profile perpendicular to the ZMP fault system as a function of the distance to the ZMP fault system (Fig. 7), we see a clear offset of up to 1 s at the location of the ZMP fault system. For stations located on the Makran block, we observe a decrease with the distance to the ZMP fault system, which is also related to a southeastward orientation of the profile. Because the crustal structure is 3D, and the slab is dipping northward beneath the Makran, it is likely that the offset decreases southward. The strong offset exactly related to the ZMP fault system, however, indicates a strong velocity contrast between the Zagros and Makran.

Yamini-Fard (2003) also computed teleseismic receiver functions. The P–S converted phases usually image the Moho discontinuity well. Their interpretation is not straightforward: the receiver function data are complex and cannot be easily used to draw a Moho profile. This complexity prob- ably comes from the departure of the flat-layered

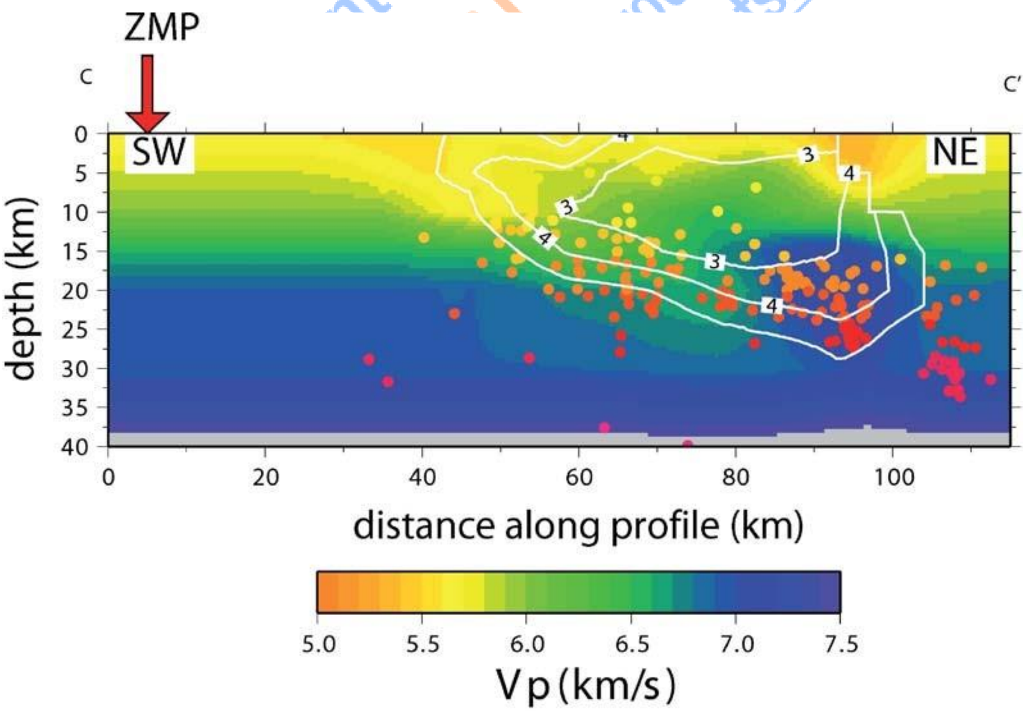

Fig. 8. Cross-section of the 3D velocity structure trending SW–NE computed from local travel-time residuals (see Fig. 3 for location.) Results are reliable for a spread function ,5 (white contour). The hypocentres are reported. There is a clear indication of a northward dipping anomaly related to the seismicity (Yamini-Fard *et al.* 2007).

structure that is used as an initial model and generates complex wave propagations in the crust.

Finally, Yamini-Fard *et al.* (2007) computed a local 3D crustal velocity structure and relocated simultaneously the local earthquakes inverting the travel times of local seismicity (Yamini-Fard *et al.* 2007). The resulting velocity structure suggests a high-velocity body dipping northeastward (Fig. 8). An important result is that no seismicity appears to be associated with the Zendan–Minab–Palami fault system, suggesting that the transition between the Zagros collision and the Makran subduction is not associated with a sharp transform fault. Instead, it is associated with a progressive transition located in the lower crust. The shallow right-lateral strike-slip faulting is the response of the upper crust to the shortening. This ‘partitioning’ in depth is probably related to the difference in the strength of the upper and lower crusts.

Modern kinematics

GPS. Vernant *et al*. (2004; updated by Masson *et al.* 2007) used a network of 27 GPS sites to establish the current large-scale deformation rates within Iran. The network was measured three times, during September 1999, October 2001 and October 2005. This work provided a useful overview of Iranian geodynamics. The researchers then divided Iran into various rigid blocks. They concluded that, to the west, the Zagros is undergoing 9 + 2 mm a^{21} of shortening, in a direction close to north–south. To the east, the Makran subduction accommodates 19 + 2 mm a^{21} of N208E-trending convergence. The Makran–Zagros transition zone should thus accommodate some 11 + 2 mm a^{21} of right-lateral movement.

Bayer *et al.* (2006) used a denser network focused on the Zagros–Makran transition zone. It consisted of 15 stations, with an average separation of *c*. 60 km, which were measured in 2000 and 2002. The GPS-derived velocity field can be expressed in various useful frames: fixed Eurasia, fixed Central Iran or fixed Arabia (Fig. 9). When expressed in a Central Iran fixed frame, the velocity directions are more or less parallel to the convergence velocity. There is no clear divergence from the Musandam peninsula (Oman), contrary to what would be expected if Musandam was acting as an indentor, as proposed by Kadinsky-Cade & Barazangi (1982; Fig. 9).

Assuming a rigid block model, Bayer *et al*. (2006) computed the motion accommodated by the Minab–Zendan–Palami fault system. They found 15 mm a^{21} and 6 mm a^{21} for the motions parallel or perpendicular to the direction of the fault (i.e. N1608E; Fig. 9). In addition, they estimated the strike-slip motion of the Jiroft–Sabzevaran fault system (north–south-trending) to be 3.1 + 2.5 mm a^{21}. The Minab–Zendan–Palami fault system motion is estimated in its southern part, where the entire Zagros–Makran motion must be accommodated (Regard *et al.* 2004), whereas in its northern part, Zagros–Makran transition zone deformation is distributed over the two fault systems. The 15 mm a^{21} MZP fault system displacement rate must therefore encompass the 3.1 + 2.5 mm a^{21} of the Jiroft–Sabzevarn fault system calculated by Regard *et al*. (2005*a*; see below).

Geodetic data show that almost all the convergence is accommodated in the east by the Makran subduction zone, whereas only half of it is accommodated in the west by the Zagros. The Zagros–Makran transition zone clearly accommodates *c.* 15 mm a^{21} of differential motion; the transpressive character of the transition zone is because of the fault obliquity relative to the overall plate convergence direction. Geodesy does not provide evidence of a rigid indentation of the Musandan peninsula into Iran, which would be represented by a velocity field pattern divergent from the Musandam peninsula.

Tectonics and geomorphology. As described above, Regard *et al*. (2004) provided evidence of two fault systems accommodating the relative velocities in the northern part of the study area (whereas the results of Bayer *et al*. (2006) concern the southern part of the system). Tectonic and geomorphological analyses combined with cosmogenic nuclide-dating (^{10}Be) have revealed a total right-lateral slip rate of 4.7 + 2.0 mm a^{21} to 6.3 + 2.3 mm a^{21} for the ZMP fault system, depending on the ages of offsets, and 5.7 + 1.7 mm a^{21} for the JS fault system (table 3 of Regard *et al.* 2005*a*; see also Regard *et al.* 2006). Regard *et al*. evaluated the total motion accommodated across the area to be 11.3 + 3.9 mm a^{21} or 13.1 + 4.3 mm a^{21} in a direction N10 + 208E.

The total shortening at the west front of the ZMP fault system is estimated to be *c*. 6 km (Fig. 4) since the Mio-Pliocene (*c*. 5 Ma, Molinaro *et al.* 2005*a*), and implies an average shortening rate of the order of 1 mm a^{21}.

Discussion

The work presented here is a compilation of data collected by various means. It gives a unique insight into the current dynamics of a subduction–collision transition zone. In particular, important questions arise, such as: What is the lithospheric structure? Where is the main structure? Does the Musandam peninsula act as an indentor? To give a coherent view of this transition we first describe what we do know about its structure, then try to

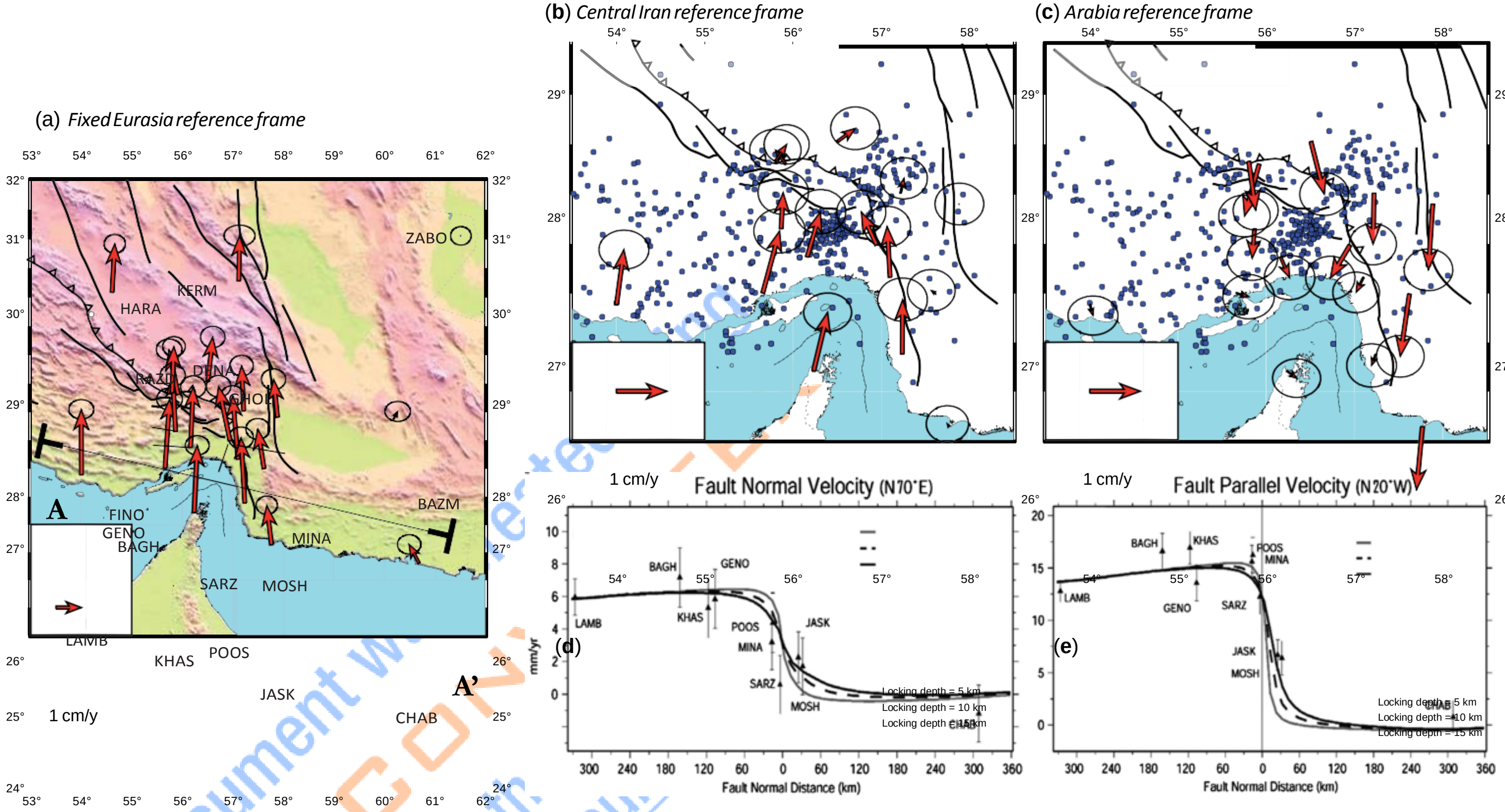

Fig. 9. GPS data for the study area (Bayer *et al.* 2006). (a) GPS velocities and their 95% confidence ellipses in a fixed Eurasia reference frame. (b, c) Detailed view of the study area

in, respectively, a fixed Central Iran reference frame and a fixed Arabia reference frame; dots represent instrumental seismicity. (d, e) GPS velocity profiles, normal and perpendicular, respectively, to the Zendan–Minab fault trend [A–A′ in (a)]. Lines refer to best-fit deformation with a block model (see Bayer *et al.* 2006, for details).

assess the question of its modern kinematics and the timing of its set-up before inferring its future through comparison with laboratory experiments and other subduction–collision transitions.

Crustal and lithospheric structure

Before Arabia and Iran began to collide, probably in the late Oligocene, the area was occupied by a continuous subduction zone. The subduction of continental Arabia to the west led to a collision, whereas to the east the oceanic part of the Arabian plate is still subducting at present. Under the Zagros collision zone the plate probably broke and the oceanic part may have sunk deep into the mantle (Molinaro *et al.* 2005*b*). Further to the east, in the study area, it is difficult to know if the nearby Zagros underwent such a slab break-off or if the subducted slab is still attached. In particular, the transitional area is wide, which suggests a gentle transition at depth, compatible with a con- tinuous deep slab (Regard *et al.* 2005*a*, *b*). Closer to the surface, seismological data display a clear view of a NE-dipping surface (Fig. 8). This plane dips *c.* 158 and is likely to originate at the surface near the ZMP fault system (Fig. 8; Yamini-Fard *et al.* 2007). This plane is associated with significant microseismicity with NE – SW-trending P-axes, showing thrusting at depth (Fig. 6; Yamini-Fard *et al.* 2007). It would thus correspond to an active crustal-scale thrust, separating a Zagros-related part in its footwall from Makran formations in its hanging wall.

The system tectonics appears more complicated in the uppermost part. It is dominated by folds and faults organized in two fault systems: (1) the ZMP fault system to the SW; (2) the JS fault system to the NE. (1) The NNW–SSE-trending ZMP fault system is associated with en echelon folding and constitutes the lithological boundary between the Zagros and Makran (Regard *et al.* 2004). It presents high-velocity anomalies (1 s residuals, Fig. 7) (Yamini-Fard 2003). It is made up of numerous and highly segmented faults. The system's western faults dip ENE whereas the eastern ones dip WSW, giving a flower-structure-like superficial organization (Regard *et al.* 2004). This system could act as a developing crustal-scale strike-slip fault, with infilling by dense material, but these observations do not agree with the balanced cross-section, which implies an 8 km deep décollement surface that should extend a couple of kilometres eastward from the ZMP fault system. This apparent discrepancy will be resolved in the discussion below. (2) The north–south-trending Jiroft–Sabzevaran fault system does not appear to be marked by any seismicity alignment although the local seismicity level is high (Yamini-Fard 2003). The faults are strike-slip with a small component of vertical motion. The fault system is partly linked to the south with the tectonic Makran northern boundary, south of the Jaz Murian depression, and partly to the ZMP fault system (Regard *et al.* 2004). To the north the system seems to continue northward to the Nayband and Gowk faults, which mark the boundary between Central Iran and the Lut Block (Walker & Jackson 2002).

Surface structural setting and modern kinematics (map view)

The current deformation at the surface and close to the fault systems is shown by seismology and active tectonics to be caused by a NE–SW-trending main compressional direction (Regard *et al.* 2004; Yamini-Fard *et al.* 2007). Active tectonics also indicates that convergence is accommodated nearly equally by the two fault systems, the deformation being distributed within each fault system instead of being localized (Regard *et al.* 2005*a*).

On a wider scale, the palaeomagnetic data show that rotations occurred both clockwise to the east and anticlockwise to the west of the transition zone. This could indicate an indentor role of the Musandam peninsula (Aubourg *et al.* 2004, 2008). On the other hand, the GPS velocity field does not show any divergence away from the 'indentor', and this would suggest that there is no rigid indenta- tion in the area (Figs 9 & 10). Tectonic observations also do not favour the Musandam peninsula indentor hypothesis, as they indicate that the motion between Arabia and Makran is accommodated only by one transcurrent fault system (the ZMP fault system), on which all the relative motion is accommodated, as indicated by the similarity in GPS and tectonic velocities.

Indeed, the global motion accommodated by the transition zone fault systems is evaluated by GPS to be 15 mm a^{21}, close to the evaluation from tectonics of 11–13 mm a^{21}. The agreement between GPS and tectonics is not so good on the part accommodated by the Jiroft–Sabzevaran fault system, the transcurrent motion of which is evaluated to be $3.1 + 2.5$ mm a^{21} or $5.7 + 1.7$ mm a^{21}, respectively (Fig. 10). The discrepancy comes from the loss of the elastic component away from the network, the easternmost station of which is close to the Jiroft Fault, as highlighted by recent results (Peyret *et al.* 2009).

Two-stage post-Miocene evolution

Some of the studies presented here highlight a two-stage scenario for the recent (since Miocene times) evolution of the area. First, magnetic studies

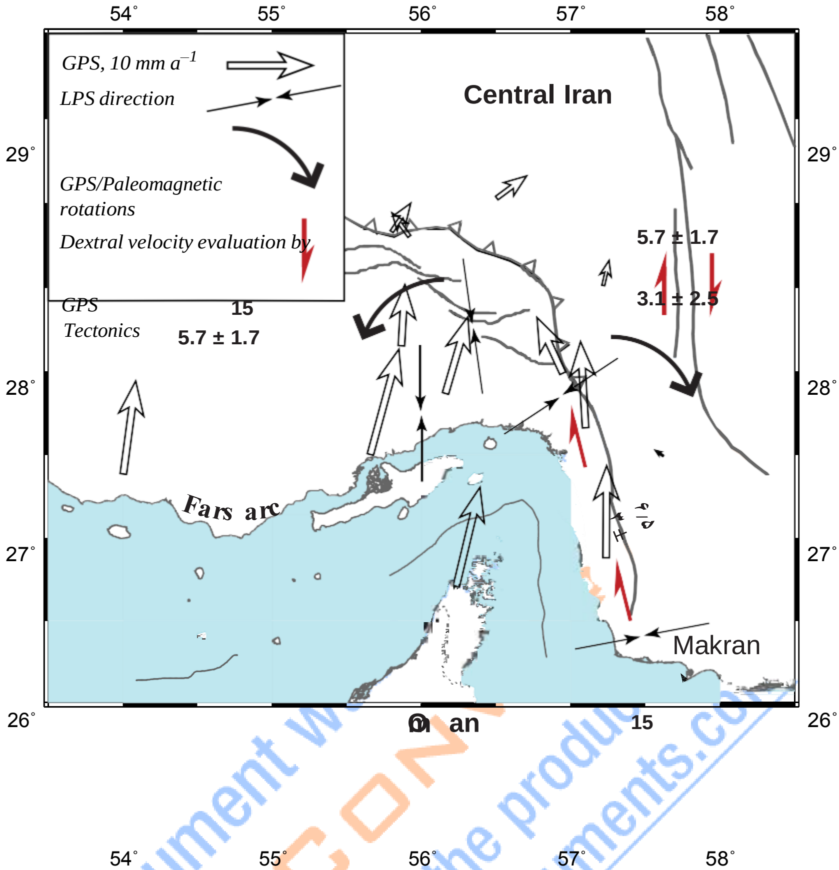

Fig. 10. Summary of observations at the surface. GPS results are indicated in a fixed Central Iran reference frame.

indicate that the transition shape, oblique to the convergence, has been acquired recently, since the Mio-Pliocene. Before the transition structural set-up, the deformation recorded by magnetism was roughly coherent with the overall plate convergence. Superimposed on this, some moderate rotations, clockwise to the east and anticlockwise to the west, may account for a slight indentation by the Musan- dam peninsula. Second, a major change in tectonics was also recorded. As emphasized above, the balanced cross-section of the Minab fold proposed by Molinaro *et al*. (2004) appears not to be compatible with modern kinematics and structure. The Minab fold may have been formed during a former deformation stage. In addition, palaeostress determinations by Regard *et al*. (2004) show a stress-orientation change in the Pliocene. Those workers suggested that it corresponds to a change from a partitioned convergence accommodation through folds and reverse faults (ZMP fault system) to non-partitioned convergence accommodation through the ZMP transpressional faulting. The best way to combine these results (tectonics, structure and kinematics) is to assume that the flat thrust shown by balanced cross-sections has been cut through by a more vertical fault, possibly evolving to a flower structure near the surface. This fault is likely to carry exotic slices such as the Palami range lying between the Palami and Zendan faults.

Comparisons with other settings, both in the laboratory and in nature

Cotton & Koyi (2000) proposed a sandbox experiment that interestingly mimics the study area although it was not intended to reproduce it (Fig. 11). The experiment comprises a sandbox undergoing north–south compression; the sand is lying over a frictional substrate in the western part whereas it is underlain by a ductile level in its eastern part (Fig. 11). Although the experiment was designed for basin tectonics, we could interpret it in terms of lithospheric structure. The frictional
v. ductile substrate should be compared with the col- lision v. subduction convergence settings. In this experiment, the eastern range (over ductile sub- strate) extends further to the south than the western range. Between the two ranges a transfer zone is produced, which is formed by two north– south-trending strike-slip faults: (1) a southwestern one connecting the deformation zone of the western

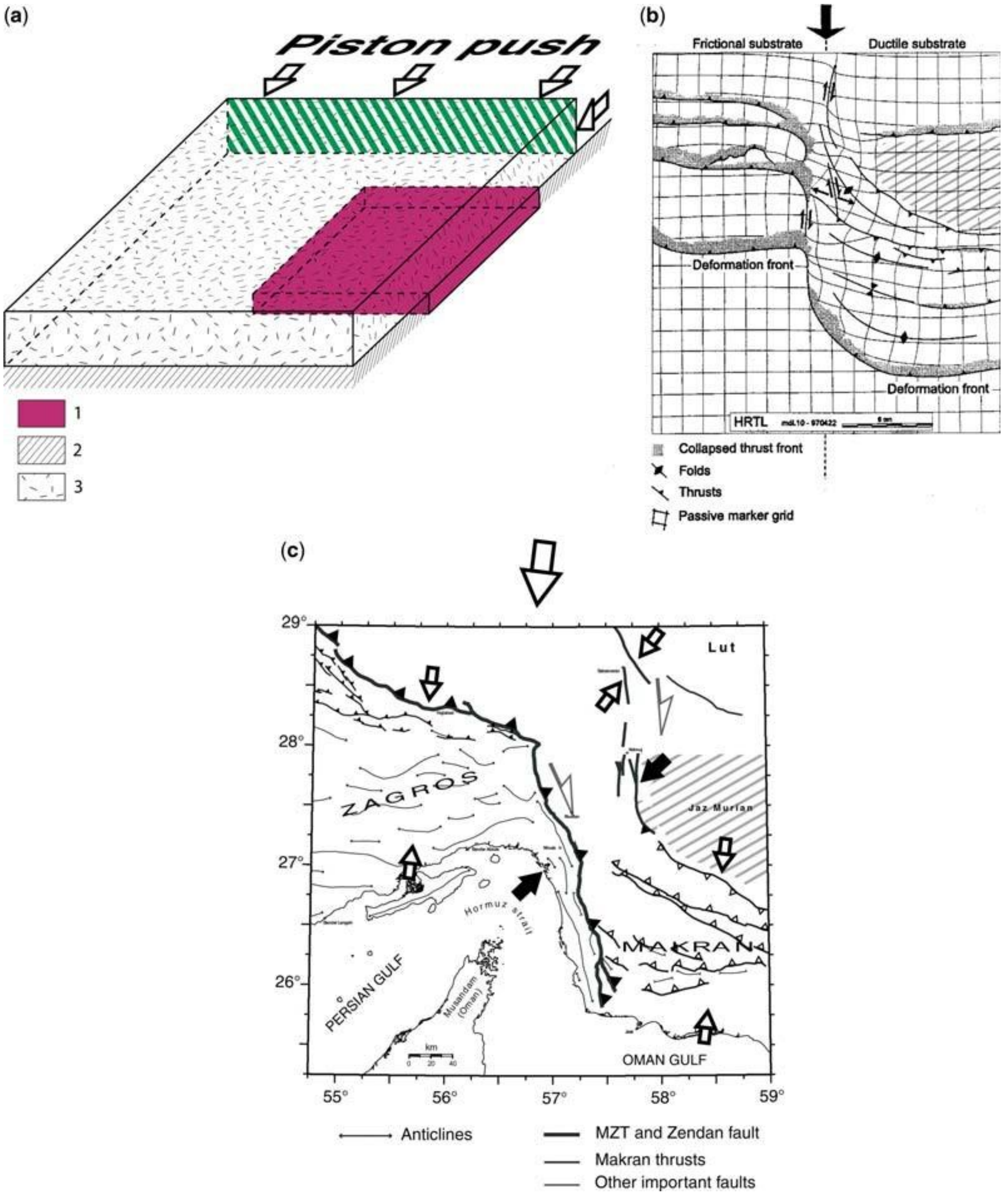

Fig. 11. Sandbox experiment by Cotton & Koyi (2000). (a) The setup consists of a box filled with sand (3) over a rigid basement (2), which is partly replaced by a low-viscosity layer (1). The sand layers experience convergence owing to piston push. (b) The experimental result shows that the structures propagate further over the viscous basement than over the rigid basement; a transition zone is created. (c) Structural scheme of our study area, with strain arrows, which resembles the experimental result (b).

range (over a frictional substrate) to the frontal thrust of the eastern one; (2) a northern one that connects the northern part of the experiment with the backstop of the eastern range (Fig. 11). Comparison of this scheme with the structural setting of the Zagros – Makran transition zone highlights many similarities; in particular, the faults (1) and (2) probably represent the ZMP and JS fault systems, respectively (Fig. 11). However, the experiment cannot explain the curvature of the Fars Arc (southeastern

Zagros); in the experiment the range over the frictional substrate has a linear trend (Fig. 11). A possible explanation for this is that in the Fars Arc the curvature is due to the underthrusting of the Musandam peninsula.

Another transition between subduction and collision can be found at the other end of the Makran. Some of us have already initiated discussion on this subject (Regard *et al.* 2005*a*). There, the transfer zone is formed by three single faults, the Chaman, Ghazaband and Ornach-Nal faults (Fig. 12). The system connects the Makran accretionary prism to the Pamirs (Panjshir Fault) (Lawrence *et al.* 1992). The overall system is thought to accommodate between 25 and 35 mm a^{21} according to geological evidence (Beun *et al.* 1979), or 40 mm a^{21} according to the NUVEL-1 model (DeMets *et al.* 1990). The most important part of the deformation is transmitted to the inner Makran and there is no evidence of active deformation transmission to the frontal, offshore, Makran thrust. The transition zone is more mature than the Zagros–Makran transition zone. Indeed, it is known to be much older (20–25 Ma instead of 5 Ma or less) and its length (more than 1000 km) implies a considerable slab stretching such that the slab must no longer be continuous between the Makran and Pamirs. Consequently, this system could be viewed as a possible future for our study area. In particular, it is noteworthy that the accommodation by two or three disconnected systems characterizes the transition zone as well as in the Cotton & Koyi (2000) experiment and at the Zagros–Makran transition (Figs 11 & 12). Some partitioning also occurs; for example, between the Chaman strike-slip fault and the Sulaiman fold belt (Lawrence *et al.* 1992; Davis & Lillie 1994). In turn, the maturity is expressed by the localization of the deforming structures, which are long, low-segmented faults in contrast to the highly segmented fault systems in the Zagros–Makran area (Regard *et al.* 2005*a*).

Synthesis

The evolution of the Zagros–Makran transition zone has probably been influenced by an inherited structural setting. For a better understanding of the way it has recently evolved, a simplified scen- ario is proposed in Figure 13. The way in which this area is deforming is comparable with both the Makran–Pamir transition and the laboratory experiment. Two characteristic fault systems are found to the SW (Zendan–Minab–Palami fault system) and NE (Jiroft–Sabzevaran fault system). To the east the Makran deformation shows the same pattern as in the experiment and at the eastern Makran boundary, but to the west, the Fars Arc shape disagrees with the experiment. We hypothesize that this is due to the complexity introduced by the Musandam peninsula, which is topographically much higher than the surrounding parts of Arabia.

The first fault system (the ZMP fault system) currently trends N1608E, oblique to the convergence. It is made up of three highly segmented faults that are the possible expression at the surface of a flower structure that changes to an oblique thrust at its northern boundary. Seismology indicates that it is correlated with a strong discontinuity at depth and that near its northern termination its deep structure is a NE-dipping plane. In this scheme some 6 km structure-normal shortening occurs that could be the result of a former strain distribution or of a slight deformation partitioning, with a frontal fault accommodating up to 5 mm a^{21} of shortening, as indicated by the recent results of Peyret *et al.* (2009). The 6 km deep décollement proposed by Molinaro *et al.* (2004) may therefore now branch at depth to the flower structure. We propose that its central fault (Zendan) represents the main boundary between the Zagros and Makran.

The second fault system (the JS fault system) trends north–south. It probably connects to the north to a well-known strike-slip system bounding the Lut block to the west. To the south its deformation probably transfers partly to the northern Makran tectonic boundary and partly to the ZMP fault system, as suggested by the laboratory experiment of Cotton & Koyi (2000).

Of the *c.* 19 mm a^{21} differential convergence rate, some 3–6 mm a^{21} are accommodated by the JS fault system and *c.* 6–7 mm a^{21} in the ZMP fault system at the Minab latitude, increasing to *c.* 15 mm a^{21} to the south; this increase corresponds to the progressive deformation transmission from the JS fault system to the ZMP fault system. It should be noted that if one part of the JS-accommodated deformation is transmitted to the Makran northernmost thrust, the 15 mm a^{21} strike-slip deformation observed to the south of the ZMP fault system is not fully explained by addition of the ZMP and JS motions (maximum 13 mm a^{21}). This discrepancy is not yet resolved.

The data presented here provide evidence of post-Miocene system evolution (Fig. 13). The overall oblique structure is from a recent (less than 5 Ma) setting as indicated by magnetism and tectonics. The set-up time is contemporaneous with a major change in the Middle East tectonics and with Zagros topography-building initiation (Allen *et al.* 2004). During this set-up, the Zagros and Makran, which were originally continuous, differentiated. Interestingly, this differentiation occurred at the time when deformation in the Zagros passed from thin-skinned to thick-skinned (Molinaro *et al.* 2004); this is very different from the Makran,

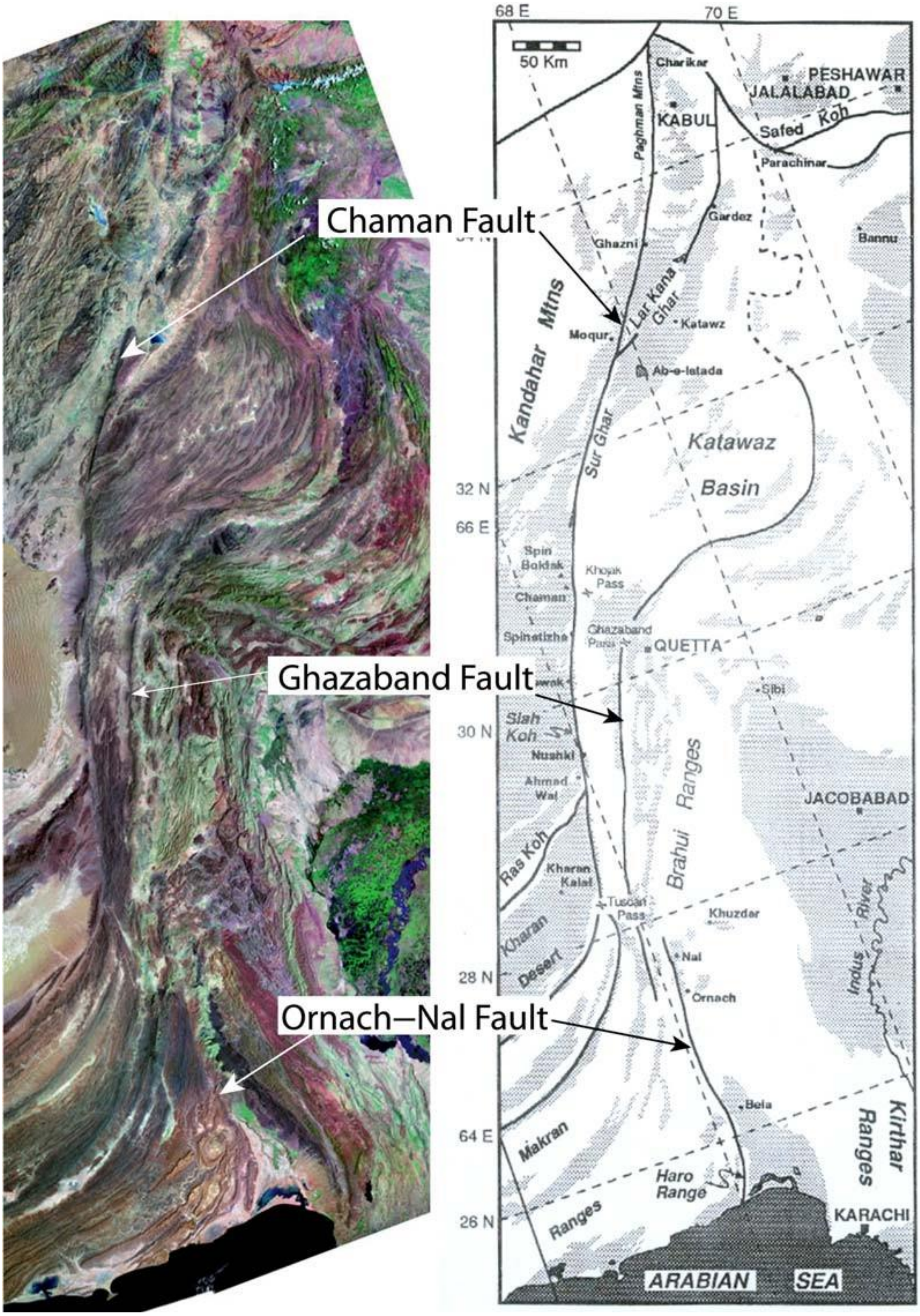

Fig. 12. Landsat image of the Chaman Fault (bands 7, 4 and 2) and its tectonic interpretation, after Lawrence *et al.* (1992). It should be notes that the transfer zone is formed by three continuous but disconnected faults: the Chaman, Ghazaband and Ornach–Nal faults.

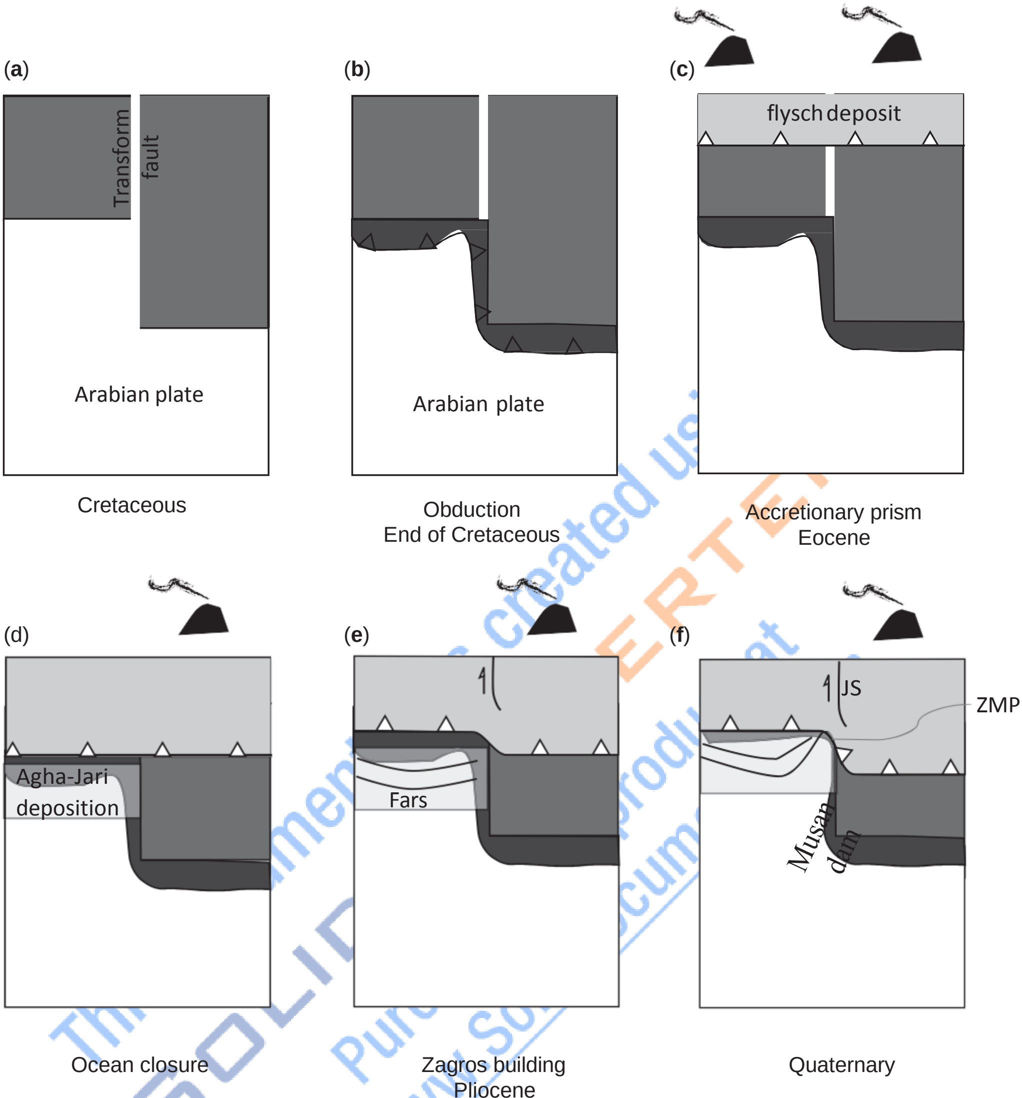

Fig. 13. Sketch of the study area history. (a) Initial setting: a former passive margin south of the Tethys, cut by a transform fault. (b) Obduction occurred near the end of the Cretaceous. (c) The Tethys northern margin had been subducting for some time when the accretionary prism began to be built (Eocene). (d) After ocean closure and emergence, the Agha-Jari formation was deposited. (e) Zagros mountain building during the Pliocene; onset of Zagros–Makran syntaxis. (f) Present setting: JS and ZMP are, respectively, the Jiroft–Sabzevaran and Zendan–Minab–Palami fault systems. The Musandam topographic high causes the Fars Arc curvature.

where only the sediment cover is scraped off. It is tempting to relate the onset of the Zagros–Makran transition zone to the initiation of thin-skinned tectonic shortening in the Zagros, which from then on was very different from the Makran tectonic style, where only the sediments overlying the oceanic crust are affected by deformation. The faults and folds forming the system are currently in a young stage and they sometimes undergo some change, as indicated by stress tensor orientation changes. At present the system is divided into two fault systems, which will endure, whereas their internal organization will simplify to localize in a single and continuous structure, although some partitioning is likely to continue. Obviously, such a transition is a lithospheric-scale deformation zone.

Conclusion

This review of studies on the Zagros–Makran tran- sition zone clarifies many points, giving a coherent overview of its structural setting and behaviour.

(1) The location of this transition is dictated by the past. Indeed, it corresponds to a coastline offset by a transform fault at the time of ocean opening (Fig. 13a).

(2) There is no evidence that currently the two deformation zones, the Zagros and Makran, are con- nected by a transform fault. Numerous faults accom- modate the deformation, organized in two fault systems. Some of the faults could be of crustal extent.

(3) The current stress state is transpressional with a NE–SE-trending σ_1; the associated strain is strike-slip with some transpressional component.

(4) An important change in tectonic style occurred at some time in the Mio-Pliocene, contem- poraneous with other changes widely recorded in the Middle East, and in the Zagros in particular. This may indicate the initiation of the zone as a transform zone between the Zagros and Makran, which from then on evolved differently (Fig. 13b–d). This initiation may be closely related to the change from thin-skinned to thick-skinned tectonics at the same time in the Zagros, whereas in Makran tec- tonics remained unchanged.

(5) At depth, a northeastward dipping plane is linked to the Zagros; this is probably an underthrust slice. This plane seems to connect to the Zendan Fault at the surface.

(6) An important clue is whether Musandam (Oman) acts as an indentor. Our conclusion is that there is no first-order indentation (Fig. 13e). How- ever, it could be a second-order indentation explain- ing the modern Fars Arc curvature (Fig. 13f).

(7) Laboratory experiments and a real-world analogue help us to imagine the future of such a transform zone: the fault zones are likely to simplify in locating the deformation in a single low- segmented fault. There is no clear evidence at present, however, that the fault zones will coalesce into a single one.

The tectonic study is indebted to the ISIS programme for SPOT satellite image acquisition (©CNES 2004 to 2007, distribution SPOT images S. A.). We wish to thank R. Walker and an anonymous reviewer for their construc- tive reviews. This work benefited from a 10 year collabor- ation between Iranian and French scientists, who all participated in data collection and discussions.

References

ALAVI, M. 1994. Tectonics of the Zagros orogenic belt of Iran: new data and interpretations. *Tectonophysics*, 229, 211–238.

Allen, M., Jackson, J. & Walker, R. 2004. Late Cenozoic reorganization of the Arabia–Eurasia collision and the comparison of short-term and long-term defor- mation rates. *Tectonics*, 23, TC2008, doi: 10.1029/ 2003TC001530.
Aubourg, C. & Robion, P. 2002. Composite ferromag- netic fabrics (magnetite, greigite) measured by AMS and partial AARM in weakly strained sandstones from western Makran, Iran. *Geophysical Journal International*, 151, 729–737.
Aubourg, C., Smith, B. *et al*. 2004. Post-Miocene shortening pictured by magnetic fabric across the Zagros–Makran syntaxis. *In*: Sussman, A. J. & Weil, A. B. (eds) *Orogenic Curvature: Integrating Paleomagnetic and Structural Analyses*. Geological Society of America, Special Papers, 383, 17–40.
Aubourg, C., Smith, B., Bakhtari, H. R., Guya, N. & Eshraghi, A. 2008. Tertiary block rotations in the Fars Arc (Zagros, Iran). *Geophysical Journal Inter- national*, 173, 659–673.
Averbuch, O., Frizon de Lamotte, D. & Kissel, C. 1992. Magnetic fabric as a structural indicator of the deformation path within a fold–thrust structure: a test case from the corbières (NE Pyrenees, France). *Journal of Structural Geology*, 14, 461–474.
Bakhtari, H. R., de Lamotte, D. F., Aubourg, C. & Hassanzadeh, J. 1998. Magnetic fabrics of Tertiary sandstones from the Arc of Fars (Eastern Zagros, Iran). *Tectonophysics*, 284, 299–316.
Bayer, R., Shabanian, E. *et al*. 2003. Active deformation in the Zagros–Makran transition zone inferred from GPS measurements in the interval 2000–2002 (abstracts EGS 2003). *Geophysical Research Abstracts*, 5, 05891.
Bayer, R., Chery, J. *et al*. 2006. Active deformation in Zagros–Makran transition zone inferred from GPS measurements. *Geophysical Journal International*, 165, 373–381.
Berberian, M. & King, G. C. P. 1981. Towards a paleo- geography and tectonic evolution of Iran. *Canadian Journal of Earth Sciences*, 18, 210–265.
Beun, N., Border, P. & Carbonnel, J. 1979. Premières données quantitative relatives au coulissage du décrochement de Chaman (Afghanistan du sud-est). *Comptes Rendus de l' Académie des Sciences*, 288, 931–934.
Blanc, E. J.-P., Allen, M. B., Inger, S.& Hassani, H. 2003. Structural styles in the Zagros Simple Folded Zone, Iran. *Journal of the Geological Society, London*, 160, 401–412.
Byrne, D. E., Sykes, L. R. & Davis, D. M. 1992. Great thrust earthquakes and aseismic slip along the plate boundary of the Makran subduction zone. *Journal of Geophysical Research*, 97, 449–478.
Carbon, D. 1996. *Tectonique post-obduction des mon- tagnes d'Oman dans le cadre de la convergence Arabie–Iran*. PhD thesis, Université Montpellier II.
Cotton, J. T. & Koyi, H. A. 2000. Modeling of thrust fronts above ductile and frictional detachments: Appli- cation to structures in the Salt Range and Potwar Plateau, Pakistan. *Geological Society of America Bulletin*, 112, 351–363.
Davis, D. M. & Lillie, R. J. 1994. Changing mechanical response during continental collision: active examples